J Fluoresc (2015) 25:403–408
DOI 10.1007/s10895-015-1527-z

ORIGINAL PAPER

Development of a Nile-Blue Based Chemodosimeter for Hg^{2+} in Aqueous Solution and its Application in Biological Imaging

Mingming Hu · Jianhua Yin · Yahong Li · Xiaofang Zhao

Received: 31 October 2014 / Accepted: 20 January 2015 / Published online: 10 February 2015

Abstract A Nile blue-based chemodosimeter was newly synthesized. It can detect Hg^{2+} in aqueous solution based on desulfurization reaction. Upon its addition into aqueous Hg^{2+} ion solution, it exhibited a considerable blue-shift in its absorption and obvious fluorescence quenching. The detection mechanism was proved by mass spectrometry analysis and Gaussian calculations. Detection at an emission of 685 nm was extremely sensitive, with a detection limit of 2.5×10^{-9} mol/L. The fluorescent images in living cells and zebrafish demonstrate its potential for studying the accumulation of mercury species in organism.

Keywords Chemodosimeter · Fluorescent probe · Hg^{2+} detection · Nile-blue

Introduction

The development of molecular-recognition and sensing systems for ions and biomolecules has received considerable attention in recent years [1–3]. Among the different ions, mercury, widely known as one of the most toxic and environmentally widespread metals, is an attractive target for sensor designs. Mainly caused by its expanded use in industry and agriculture [4], it's widespread in the lithosphere and in water. It accumulates in the food chain and reaches the human body mainly through food ingestion (in particular seafood), thus causing dangerous conditions of intoxication and a variety of serious metabolic, cognitive, and motor disorders, and sensory long-term diseases [5, 6].

Relative to traditional detection methods for the quantitative analysis of ions, such as atomic absorption spectroscopy, cold-vapour atomic fluorescence spectrometry, and gas chromatography, fluorescence detection has been proved to be the most convenient method owing to its simplicity and sensitivity [7–9]. Therefore, the detection of mercury by fluorescence sensors has been a popular subject in host/guest chemistry and supramolecular chemistry in the past two decades [10–12]. Because of the thiophilicity of mercury, the identification of these probes is mostly based on the mechanism of coordination. It enhances the complexing ability of Hg^{2+} and ligand, but also reduces the selectivity of ligand, because usually, the ligands can also be coordinated with Pb^{2+} and Ag^{+} ions. Compared with coordination-based sensors, chemodosimeters based on specific reaction, are very advantageous in terms of selectivity and sensitivity, as they can effectively avoid the interference of other environmental factors in the detection [13, 14].

No matter which type of fluorescent probes as used, all the structures are mostly based on the connection of fluorophore and recognition sites, through an appropriate connection arm. During the design process, we aimed for effective stacking of the two parts (that is the fluorescent signal of fluorophore and complexing capability of recognition site). However, due to problems caused by the practical stereo-hindrance and the electronic density, it was difficult for the aim to be met. After combination, the nature of these two functional groups could not be properly preserved. For example, because of Intramolecular Charge Transfer, quenched before recognition [15, 16]; and, in different detection systems, the metal ion ligand was

Electronic supplementary material The online version of this article (doi:10.1007/s10895-015-1527-z) contains supplementary material, which is available to authorized users.

M. Hu (✉) · J. Yin · Y. Li · X. Zhao
The Institute of Seawater Desalination and Multipurpose Utilization, SOA, Tianjin, China
e-mail: mmhu_sdmu@126.com

sensitive to pH [17, 18]. These problems also exist in chemodosimeters, a typical example is a mercury ion ligand used in detection of $H_2PO_4^-$ [19] (example 33).

With such problems at the forefront, we have focused on the synthesis of a new derivative of Nile blue, NBHg-1, which has distinguished properties of near infrared excitation and emission, high fluorescent quantum yields, and exceptional stability against photo-bleaching [20]. We investigated its chemodosimetric properties which can provide sensitive measurements of Hg^{2+} ion in aqueous environments. Its application in living Hela cells and zebrafish was also being studied.

Materials and Methods

Materials

All the chemicals and solvents were of analytical reagents. The solutions of metal ions were prepared from the hydrochloride of Na^+, Ca^{2+}, Mg^{2+}, K^+, Cd^{2+}, Mn^{2+}, Cr^{3+}, Co^{2+}, Zn^{2+}, Cu^{2+}, Pb^{2+}, Hg^{2+}, natrite salt of Ag^+, and the sodium salts of HPO_4^-, SO_4^{2-}, NO_3^-, Cl^-, HCO_3^-, NO_2^-, CO_3^{2-}, SO_3^{2-} respectively. The whole salts were then dissolved in distilled water.

^{1}H-NMR and ^{13}C-NMR spectra were recorded on a VARI AN INOVA-400 spectrometer, chemical shifts reported as ppm (in $CDCl_3$ or CD_3OD, TMS as internal standard). Mass spectrometry data were obtained with a HP1100LC/MSD mass spectrometer and a LC/Q-TOF MS spectrometer. Fluorescence measurements were performed on a VARIAN CARY Eclipse Fluorescence Spectrophotometer (Serial No. FL0812-M018). Absorption spectra were measured on Unico UV/VIS UV-2102 spectrophotometer. All pH measurements were made with a Model PHS-3C meter.

Synthetic Procedures

To a cold solution of 5-(diethylamino)-2-nitrosophenol (0.20 mg, 1.11 mmol) in ethanol (2 ml), naphthalene derivative (0.40, 1.11 mmol), concentrated hydrochloric acid (1 ml) was added. The mixture was refluxed for 4 h and monitored by TLC. The solvent was removed under reduced pressure and the crude mixture was purified by column chromatography (silica, methylene chloride/methanol, 10:1) to give NBHg-1 as a metalescent green solid (0.47 g, 85 %). ^{1}H-NMR(400 MHz, CD_3OD), δH (ppm): 8.93(d, 1H, *J*=8 Hz), 8.37(d, 1H, *J*=8 Hz), 7.92 (t, 2H, *J*=8 Hz), 7.83(t, 1H, *J*= 8 Hz), 7.31(t, 3H, *J*=8 Hz), 7.20(m, 4H, *J*=8 Hz), 6.93(s, 1H), 4.08(t, 2H, *J*=8 Hz), 3.99(t, 2H, *J*=8 Hz), 3.72(m, 4H, *J*= 8 Hz), 3.60(m, 1H, *J*=8 Hz), 1.35(t, 6H, *J*=8 Hz), 1.18(t, 1H, *J*=8 Hz); ^{13}C-NMR(100 MHz, CD_3OD), δC(ppm):181.83, 158.49, 154.42, 151.73, 148.48, 137.66, 131.57, 130.54, 129.44, 128.95, 124.41, 124.14, 123.23, 122.81, 115.57, 95.44, 93.31, 45.69, 44.42, 42.31, 11.57; TOF MS(ES):m/z Calcd for $C_{29}H_{30}N_5OS^+$:496.2171, Found: 496.2166.

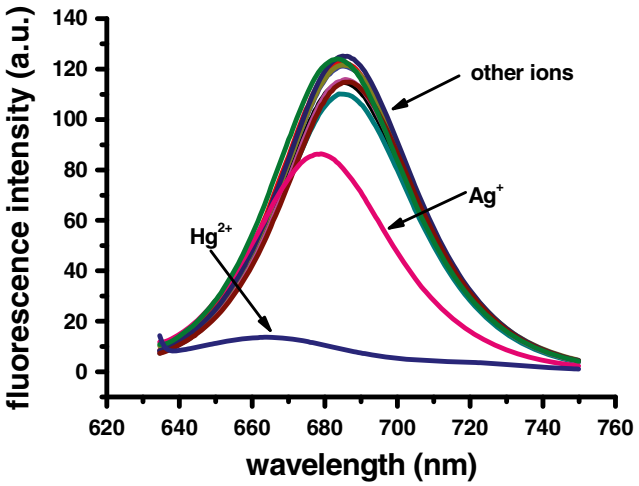

Fig. 1 Fluorescence responses of NBHg-1 (5 μM) measured in aqueous solution buffered in pH 7.4 (HEPES, 20 mM; $NaNO_3$, 100 mM; pH 7.4) with 5 equiv. of respective ions

General UV–Vis Fluorescence Spectra Measurements

Since the chemosensor was fully soluble in 100 % aqueous media, stock solution of NBHg-1 was prepared in distilled water. The UV–vis and fluorescence spectra were obtained in C_2H_5OH/HEPES (20 mM HEPES, 100 mM $NaNO_3$, 1/1, *v*/*v* pH 7.4) solution.

Determination of the Detection Limit

The detection limit was calculated based on the method used in the previous literature [21]. The fluorescence emission

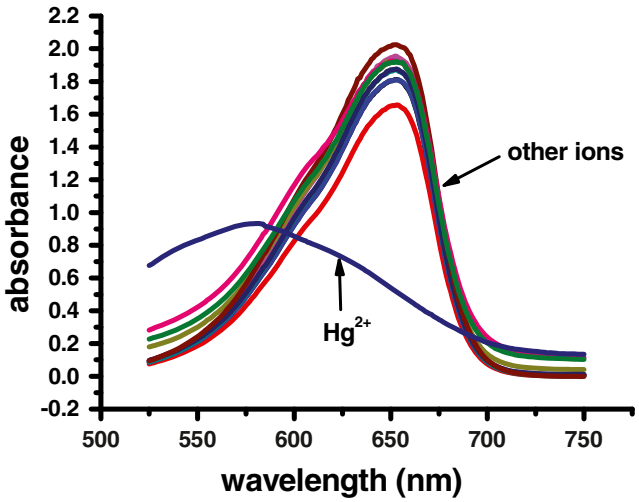

Fig. 2 Absorption responses of NBHg-1 (5 μM) measured in aqueous solution buffered in pH 7.4 (HEPES, 20 mM; $NaNO_3$, 100 mM; pH 7.4) to various ions

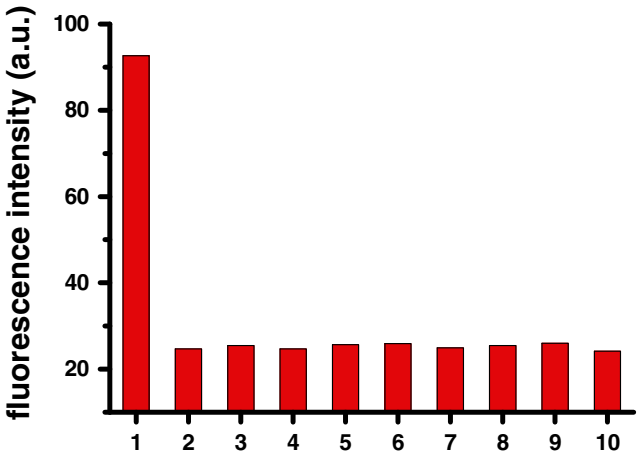

Fig. 3 Fluorescence responses (λ_{em}=685 nm) of NBHg-1 (5 μM) measured in a aqueous solution buffered in pH 7.4 (HEPES, 20 mM; $NaNO_3$, 100 mM; pH 7.4) with 5 equiv. of Hg^{2+} and then various anions (5 equiv.) 1. NBHg-1; 2. NBHg-1+Hg^{2+}; 3. NBHg-1+Hg^{2+}+$HPO_4 2^-$; 4. NBHg-1+Hg^{2+}+SO_4^{2-}; 5. NBHg-1+Hg^{2+}+NO_3^-; 6. NBHg-1+Hg^{2+}+Cl^-; 7. NBHg-1+Hg^{2+}+HCO_3^-; 8. NBHg-1+Hg^{2+}+NO_2^-; 9. NBHg-1+Hg^{2+}+CO_3^{2-}; 10. NBHg-1+Hg^{2+}+SO_3^{2-}

spectrum of NBHg-1 was measured by three times and the standard deviation of blank measurement was achieved. The fluorescence intensity at 685 nm was plotted as a concentration of Hg^{2+}. The detection limit was calculated with the following equation:

$$\text{Detection limit} = 3\sigma/k$$

Where σ is the standard deviation of blank measurement, k is the slope between the fluorescence intensity versus Hg^{2+} concentration.

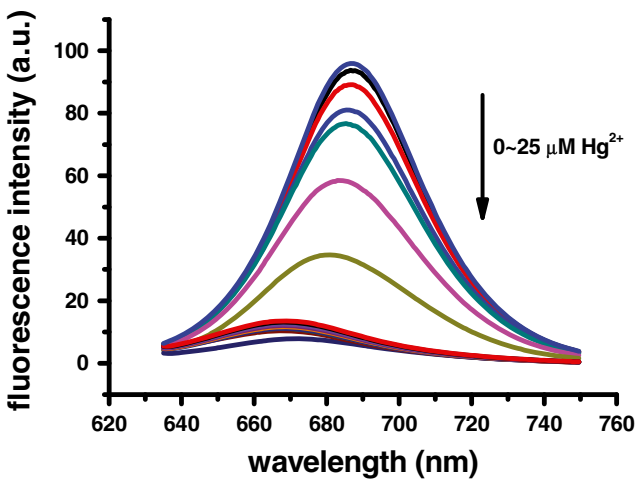

Fig. 4 Fluorescence responses of NBHg-1 (5 μM) measured in a aqueous solution buffered in pH 7.4 (HEPES, 20 mM; $NaNO_3$, 100 mM; pH 7.4) to various concentrations of Hg^{2+} (0, 0.1, 0.2, 0.3, 0.5, 0.7, 1, 2, 3, 4, 5, 7, 10, 12, 15, 20, 25 μM)

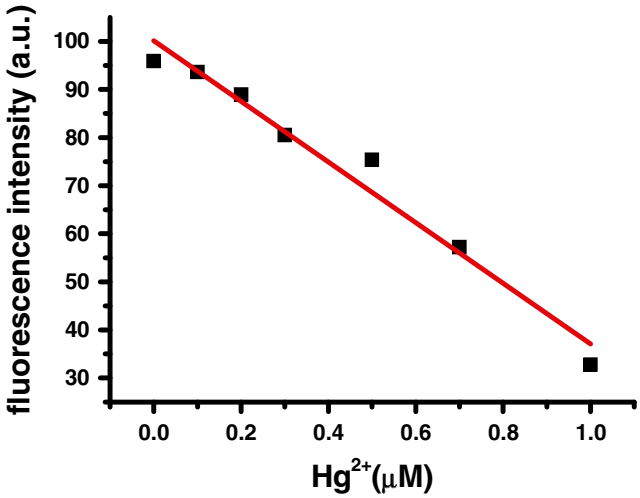

Fig. 5 The fluorescence changes at 685 nm, upon addition of lower concentrations of Hg^{2+} at 0.1-1.0 μM. λ_{ex}=610 nm

Imaging of Mammalian Cells Incubated with NBHg-1 and Hg^{2+}

Hela cells were seeded onto the cover slips at a concentration of 2×10^4 cells mL^{-1} and cultured in DMEM, supplemented with 10 % neonatal bovine serum in an incubator (37 °C, 5 % CO_2 and 20 % O_2). After 24 h, the cover slips were rinsed three times with PBS to remove the media and the cultured in PBS for later use. 10 μM of probes were added to above cellular samples and incubated for 20 min, and then the samples were slightly rinsed with PBS thrice and observed under a Leica TCS SP8 confocal fluorescence microscope. The 20 μM Hg^{2+} was added into the above cell solution, after culturing for another 20 min, and the white light and fluorescence pictures were obtained with same methods.

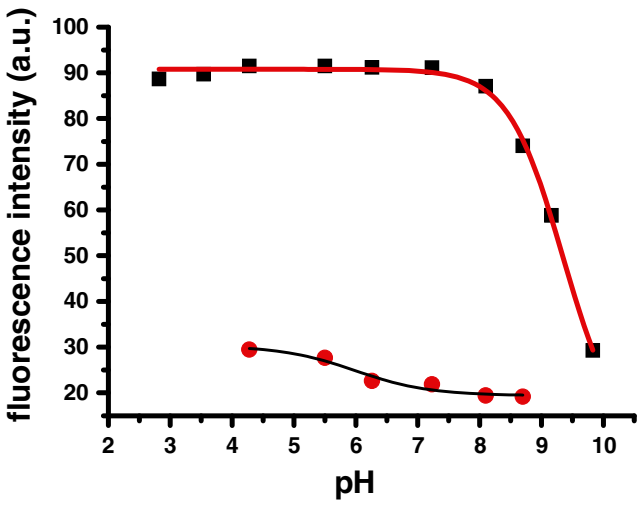

Fig. 6 Effect of pH on fluorescence intensity (λ_{ex}=610 nm) of NBHg-1 (5 μM) at 685 nm measured in an aqueous solution buffered in pH 7.4 (HEPES, 20 mM; $NaNO_3$, 100 mM; pH 7.4). The pH of solution was adjusted by aqueous solution of NaOH (aq, 1 M) or HCl (aq, 1 M)

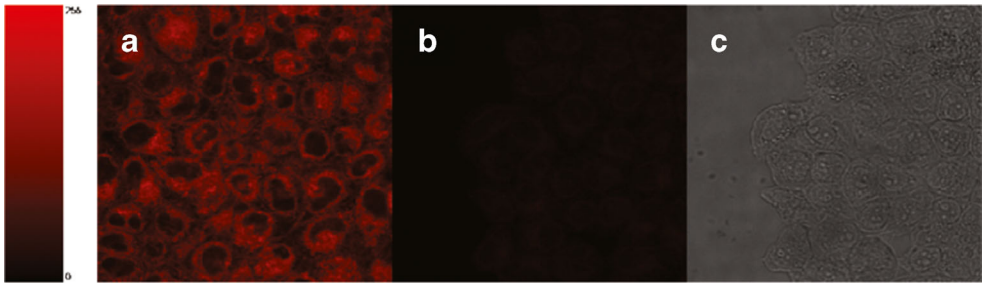

Fig. 7 Fluorescence images of Hg^{2+} ions using NBHg-1 in living Hela cells: **a** fluorescence image of living Hela cells treated with NBHg-1 (10 μM); **b** fluorescence image of NBHg-1 loaded cell exposed to 20 μM Hg^{2+}; **c** brightfield image of cells in panel **d**. Exciation: 633 nm. Emission: 685±20 nm

Imaging of Zebrafish Incubated with Chemodosimeter NBHg-1

The three-day-old zebrafish was maintained in E3 embryo media (15 mM NaCl, 0.5 mM $MgSO_4$, 1 mM $CaCl_2$, 0.15 mM KH_2PO_4, 0.05 mM Na_2HPO_4, 0.7 mM $NaHCO_3$, 10^{-5} % methlene blue; pH 7.4). The three-day-old zebrafish was incubated with 30 μM of NBHg-1 in E3 media for 30 min at 28 °C. After washing with PBS to remove the remaining probe, the zebrafish was imaged by Leica TCS SP8 fluorescence microscopy.

Quantum Calculation

The structure of NBHg-1 and the product by recognition of Hg^{2+} were calculated by DFT/TDDFT in B3LYP/6-31G level of Gaussian 09 [22].

Results and Discussion

Spectroscopic measurements for NBHg-1 were performed in aqueous solution buffered in pH 7.4 (HEPES, 20 mM; $NaNO_3$, 100 mM; pH 7.4). The response of NBHg-1 to various ions was evaluated (Fig. 1). The fluorescence emission spectrum of NBHg-1 demonstrates that Hg^{2+} could cause rapid fluorescence quenching. When 25 μM various ions were added into the 5 μM NBHg-1 solution, Hg^{2+} could induce obvious fluorescence quenching. Though Ag^{+} also caused little fluorescence changes, the intensities was far less than Hg^{2+}. Especially, we calculated the absorption changes after addition various ions (Fig. 2), and only Hg^{2+} caused a 74 nm blue shift from 650 to 576 nm. This indicated that, the fluorescence quenching by addition of Hg^{2+} was caused by change of fluorophore push-pull system instead of simple complexing.

To prove the selectivity of Hg^{2+} over other anions, we examined Hg^{2+}/anion coexisting systems. As a result, none of the common anions has distinct impact on the value of the fluorescent intensity. The competition experiment reveals that the Hg^{2+}-induced fluorescence response was unaffected by the background of common anions (Fig. 3).

We also tested the detection ability of NBHg-1 in lower concentrations of Hg^{2+} Fig. 4. As shown in Fig. 5, the fluorescence intensity decreased with the addition of Hg^{2+}. The intensities at 685 nm show a linear response to 0-1.0 μM Hg^{2+} with a detection limit at 2.5×10^{-9} mol/L based on the fluorescence titration, which reaches the standards of US EPA and World Health Organization (WHO) for drinking water (2 ppb).

As known previously, the pH-insensitivity of fluorescence in near neutral media is of importance for practical

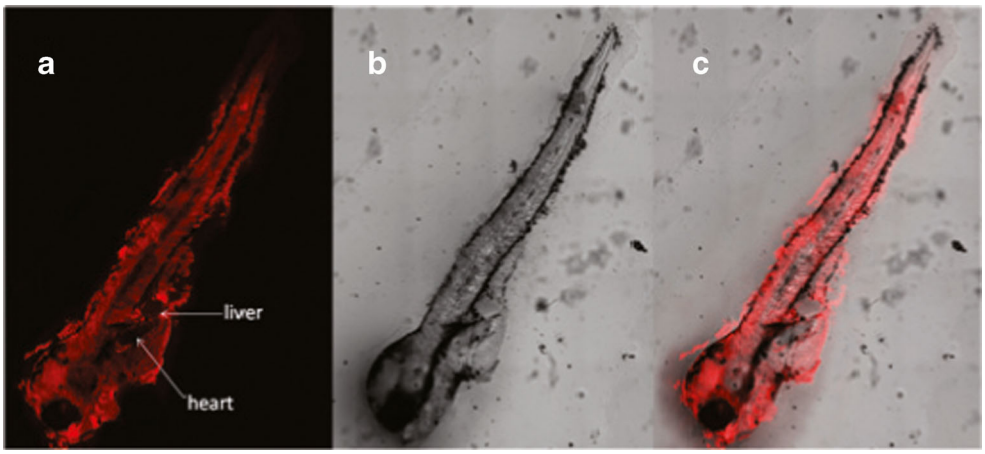

Fig. 8 Microscopic and fluorescent images of zebrafish. The three-day-old zebrafish was treated with 30 μM NBHg-1 for 30 min, washed with PBS buffer to remove the remaining chemodosimeter. Exciation: 633 nm. Emission: 685±20 nm. **a** fluorescent images of zebrafish; **b** microscopic images of zebrafish; c the overlay of (*a*) and (*b*)

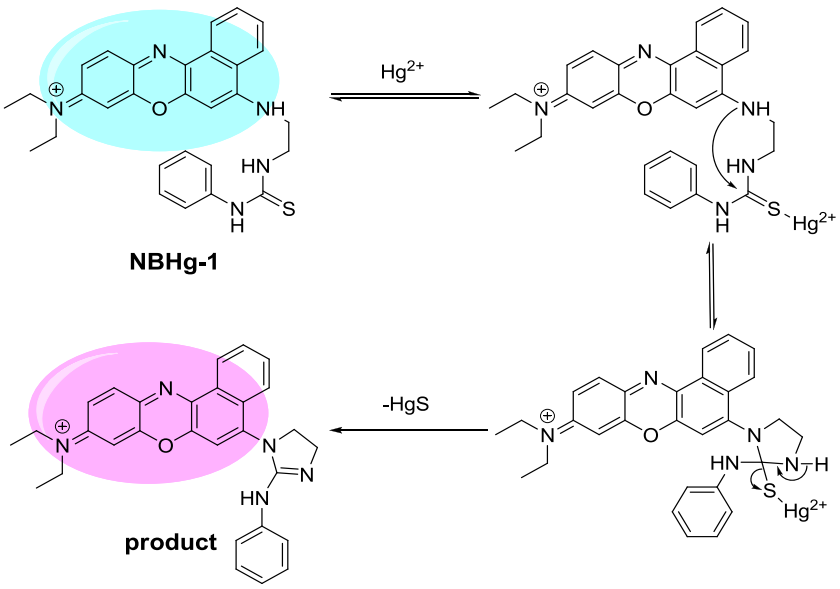

Scheme 1 Proposed mechanism for recognition of Hg^{2+} by NBHg-1

applications in both environmental and biological analyses. As seen in Fig. 6, the acid–base titration control experiments were carried out by adjusting the pH with an aqueous solution of NaOH or HCl. The pH titration curve reveals that NBHg-1 reaches almost a constant value at pH 4~8 with pK_a at 9.35 . The results demonstrate that the chemodosimeter NBHg-1 can work in a wide pH range without influence.

Figure 7 shows the fluorescence images of NBHg-1 loaded Hela cells in the absence and presence of Hg^{2+} by fluorescence confocal imaging. The Hela cells incubated with only NBHg-1 exhibited strong fluorescence signal (Fig. 7a). By contrast the cells stained with both the probe and Hg^{2+} showed an abvious fluorescence quenching in the cytoplasm (Fig. 7b), which was in accordance with the results shown in spectroscopic measurements.

To examine the fluorescent images in living organisms, three-day-old zebrafish was incubated with 30 μM of NBHg-1 for 30 min at 28 °C. After washing with PBS to remove the remaining probe, the zebrafish was imaged by Leica TCS SP8 fluorescence microscopy. From the Fig. 8, we can see the dye was distributed in the whole zebrafish evenly; the organs such as heart and liver were distinguished

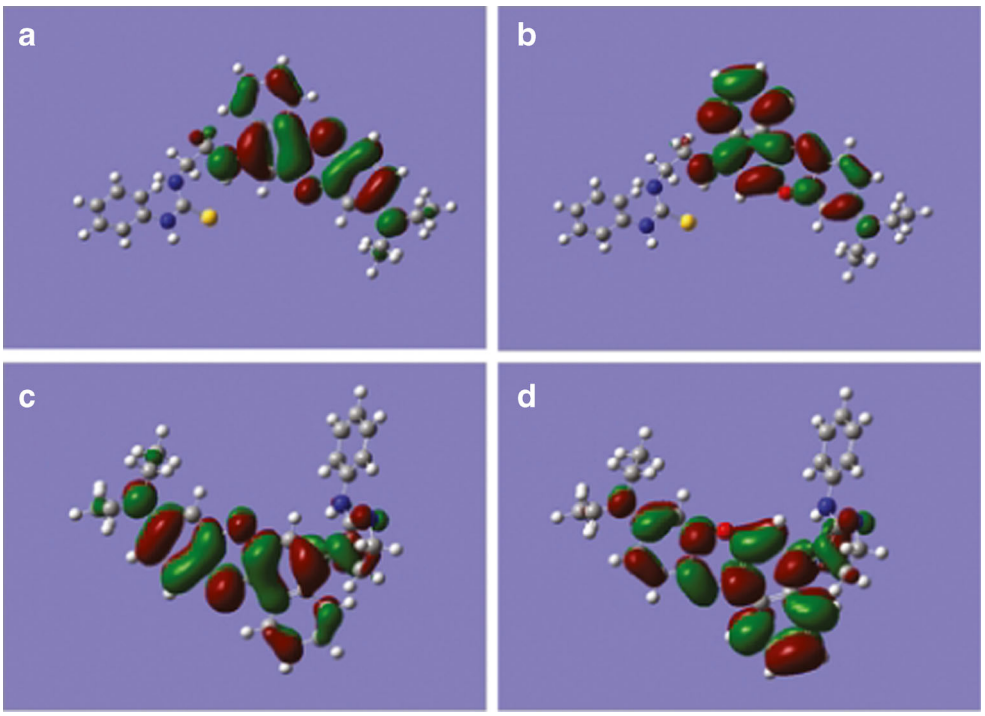

Fig. 9 Calculation of the energy level of NBHg-1 and the product reaction with Hg^{2+}. The structures were optimized by DFT/TDDFT in B3LYP/6-31 g(d,p). The HOMOs of NBHg-1 (**a**), and LUMOs of NBHg-1 (**b**), HOMOs of product (**c**), LUMOs of product (**d**)

particularly clear. The fluorescent images in zebrafish demonstrate that, the chemodosimeter has potential for studying the accumulation of mercury species in organism.

Proposed mechanism for recognition of Hg^{2+} was shown in Scheme 1, and the detection mechanism was proved by mass spectrometry analysis. The TOF-MS of the product was Calc. $C_{29}H_{28}N_5O^+$: 462.2294, and found 462.2279. (see supporting information) To explain the spectral changes of NBHg-1 by recognition of Hg^{2+}, using Gaussian 2009 (B3LYP/6-31 g(d, p)),[19] the frontier molecular orbital energy of NBHg-1 was calculated. As shown in Fig. 9, the calculations based on density functional theory (DFT) for NBHg-1 and the product were performed. Comparing the level changes of the HOMO (the highest occupied molecular orbitals) and LUMO (the lowest unoccupied molecular orbitals) in NBHg-1 and the product, respectively, after reaction with Hg^{2+}, both of them decreased due to the ICT effect. As the HOMOs decreased much more, the HOMO-LUMO energy gaps were calculated as 1.75 eV and 1.83 eV for NBHg-1 and the product, respectively, which is in agreement with the remarkable blue-shift in the absorption spectra.

The results from the spectra and the Gaussian calculation suggest that the rational design of this fluorophore can be used for designing new fluorescent chemodosimeter.

Conclusions

In summary, an example of Nile-blue based fluorescent probe, NBHg-1 was developed to detect Hg^{2+} in aqueous solution. It is a highly efficient chemodosimeter for Hg^{2+} within a pH range of 4~8 at room temperautre. In particular, the mechanism was based on Hg^{2+} induced desulfurisation followed cyclisation, which allows high sensitivity and selectivity of NBHg-1 towards Hg^{2+}. Furthermore, the spectral change was confirmed by Gaussian calculation. Hence, synthesis of NBHg-1 and its selective and sensitive Hg^{2+} detection in aqueous systems can give a potential guideline in environmental and biological application-oriented chemodosimeter research.

Acknowledgments This work was supported by the Public science and technology research funds projects of ocean (201505021–2, 201005023–4), and Youth science funds project of ocean (2013560).

References

1. Chen X et al (2010) Fluorescent and colorimetric probes for detection of thiols. Chem Soc Rev 39(6):2120–2135
2. Feng X et al (2010) Water-soluble fluorescent conjugated polymers and their interactions with biomacromolecules for sensitive biosensors. Chem Soc Rev 39(7):2411–2419
3. Xu Z, Yoon J, Spring DR (2010) Fluorescent chemosensors for Zn^{2+}. Chem Soc Rev 39(6):1996–2006
4. Vernet P (1991) Heavy metals in the environment. Elsevier, New York
5. Charlet L et al (2012) Neurodegenerative diseases and exposure to the environmental metals Mn, Pb, and Hg. Coord Chem Rev 256(19–20):2147–2163
6. Fitzgerald WF, Lamborg CH, Hammerschmidt CR (2007) Marine biogeochemical cycling of mercury. Chem Rev 107(2):641–662
7. Wade CR et al (2010) Fluoride Ion complexation and sensing using organoboron compounds. Chem Rev 110(7):3958–3984
8. Keum D, Kim S, Kim Y (2014) A fluorescence turn-on sensor for the detection of palladium ions that operates through in situ generation of palladium nanoparticles. Chem Commun 50(10):1268–1270
9. Guo Z et al (2014) Recent progress in the development of near-infrared fluorescent probes for bioimaging applications. Chem Soc Rev 43(1):16–29
10. Zhang X, Xiao Y, Qian X (2008) A ratiometric fluorescent probe based on FRET for imaging Hg^{2+} ions in living cells. Angew Chem Int Ed 47(42):8025–8029
11. Wang GK et al (2014) A pyrene derivative for Hg^{2+}-selective fluorescent sensing and its application in in vivo imaging. Chem Asian J 9(3):744–748
12. Meng Q et al (2011) A hybrid mesoporous material functionalized by 1,8-naphthalimide-base receptor and the application as chemosensor and absorbent for Hg^{2+} in water. Talanta 84(1):53–59
13. Du J et al (2012) Fluorescent chemodosimeters using "mild" chemical events for the detection of small anions and cations in biological and environmental media. Chem Soc Rev 41(12):4511–4535
14. Yang Y et al (2013) Luminescent chemodosimeters for bioimaing. Chem Rev 113:192–270
15. Hirano T et al (2000) Highly zinc-selective fluorescent sensor molecules suitable for biological applications. J Am Chem Soc 122(49): 12399–12400
16. Wang J et al (2005) A pH-resistant Zn(ii) sensor derived from 4-aminonaphthalimide: design, synthesis and intracellular applications. J Mater Chem 15(27–28):2836–2839
17. Zhang W et al (2009) A highly sensitive acidic pH fluorescent probe and its application to HepG2 cells. Analyst 134(2):367–371
18. Yuan L, Lin W, Feng Y (2011) A rational approach to tuning the pKa values of rhodamines for living cell fluorescence imaging. Org Biomol Chem 9(6):1723–1726
19. Duke RM et al (2010) Colorimetric and fluorescent anion sensors: an overview of recent developments in the use of 1,8-naphthalimide-based chemosensors. Chem Soc Rev 39(10):3936–3953
20. Fan J et al (2014) Fluorescence imaging lysosomal changes during cell division and apoptosis observed using Nile blue based near-infrared emission. Chem Commun 50(7):882–884
21. Zhu B et al (2011) A 4-hydroxynaphthalimide-derived ratiometric fluorescent chemodosimeter for imaging palladium in living cells. Chem Commun 47(30):8656–8658
22. Frisch MJ, Trucks GW, Schlegel HB, Scuseria GE, Robb MA, Cheesseman JR, Scalmani G, Barone V, Mennucci B, Petersson GA, Nakatsuji H, Caricato M, Li X, Hratchian HP, Izmaylov AF, Bloino J, Zheng G, Sonnenberg JL, Hada M, Ehara M, Toyota K, Fukuda R, Hasegawa J, Ishida M, Nakajima T, Honda Y, Kitao O, Nakai H, Vreven T, Montgomery JA Jr, Peralta JE, Ogliaro F, Bearpark M, Heyd JJ, Brothers E, Kudin KN, Staroverov VN, Kobayashi R, Normand J, Raghavachari K, Rendell A, Burant JC, Iyengar SS, Tomasi J, Cossi M, Rega N, Millam JM, Klene M, Knox JE, Cross JB, Bakken V, Adamo C, Jaramillo J, Gomperts R, Stratmann RE, Yazyev O, Austin AJ, Cammi R, Pomelli C, Ochetershk JW, Martin RL, Morokuma K, Zakrzewshi VG, Voth GA, Salvador P, Dannenberg JJ, Dapprich S, Daniels AD, Farkas O, Foresman JB, Ortiz JV, Cioslowski J, Fox DJ (2009) The gaussian 09 package refer to gaussian 09, revision a.02. Gaussian, Inc, Inc., Wallingford CT